

1           System size dependence of particle production and  
2           collectivity from the STAR experiment at RHIC\*

3                           TONG LIU (FOR THE STAR COLLABORATION)

4           Wright Laboratory, Yale University, New Haven, Connecticut 06520

5                           *Received September 1, 2022*

6           Medium modification of particle spectra and the origin of collectivity in  
7           small collision systems are widely debated topics in the heavy-ion commu-  
8           nity. To address these open questions, we propose the study of particle pro-  
9           duction and collectivity for varying system sizes, Au+Au > Ru+Ru/Zr+Zr  
10          > Cu+Cu > d+Au >  $\gamma$ +Au, available at RHIC using the STAR detector.

11          We present the first measurements of centrality dependent charged  
12          hadron production in Isobar (Ru+Ru and Zr+Zr) collisions, including the  
13          nuclear modification factors ( $R_{AA}$ ) at high transverse momentum ( $p_T$ ),  
14          and identified particle spectra at low  $p_T$  at mid-rapidity. Combined with  
15          existing results from other systems, they probe system size and collision  
16          geometry dependences of the medium modification to particle production.

17          In addition, we present the measurement of particle production and  
18          long-range di-hadron correlations in  $\gamma$ +Au events using ultra-peripheral  
19          Au+Au collisions at RHIC.

20                           **1. Introduction**

21          Since the discovery of the quark-gluon plasma (QGP) [1], its various  
22          properties and how they depend on initial conditions have been under ac-  
23          tive investigation. One such effort is the beam energy scan (BES) performed  
24          by RHIC [2], which studies how QGP properties change with the collision  
25          energy. Yet, there is another equally important dimension, i.e. the system  
26          size dependence. RHIC provides a large variety of collision systems, cover-  
27          ing the number of participating nucleons ( $N_{\text{part}}$ ) from 1 to a few hundred.  
28          Furthermore, systems with similar  $N_{\text{part}}$  but different initial geometry can  
29          be used to study how medium properties evolve with the collision system.

30          In these proceedings, we present the following results from the STAR  
31          experiment. In Sec.2, we first focus on the high- $p_T$  charged hadron spectra  
32          at  $\sqrt{s_{NN}} = 200$  GeV and compare their  $R_{AA}$  in different systems, namely

---

\* Presented at Quark Matter 2022

33 Au+Au, Isobar, Cu+Cu and  $d$ +Au. In Sec.3, we focus on the 200 GeV  
 34 Isobar collision system and explore the low- $p_T$  spectra of identified charged  
 35 hadrons, especially the yield ratios between Ru+Ru and Zr+Zr. Finally, in  
 36 Sec.4, we study photonuclear events tagged in 54 GeV Au+Au collisions,  
 37 and present a study probing the long-range correlation in such events.

## 38 2. Nuclear modification of hard partons in Isobar collisions

39 In this section and Sec.3, we utilize the isobaric collision data taken  
 40 by STAR in 2018. A detailed description of the run, event, and centrality  
 41 selection can be found in Ref. [3]. The efficiency corrected mid-rapidity  
 42 ( $|\eta| < 0.5$ ) charged particle spectra are divided by the  $p+p$  spectrum scaled  
 43 by the number of binary collisions ( $N_{\text{coll}}$ ) from Ref. [4] to obtain the  $R_{AA}$ .

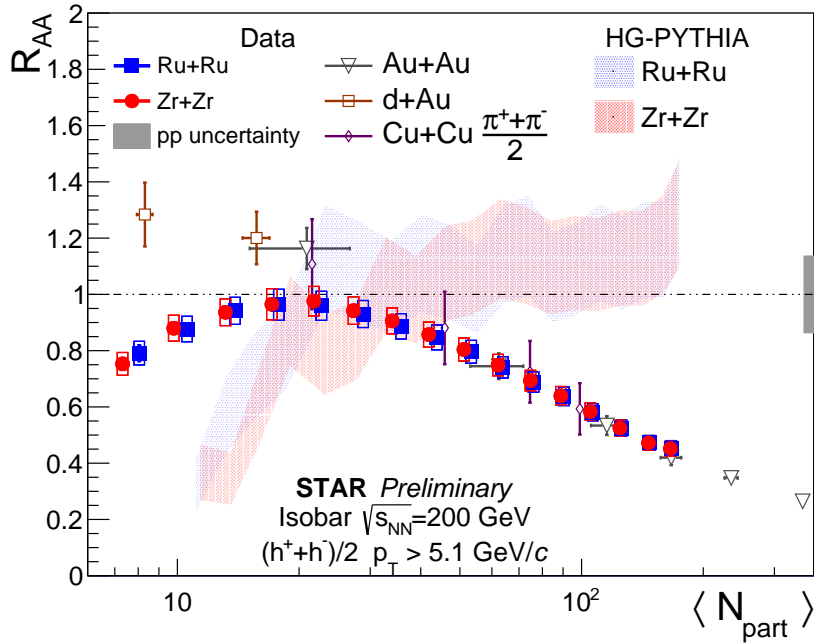


Fig.1.  $R_{AA}$  of inclusive charged hadrons with  $p_T > 5.1$  GeV/ $c$ . For the isobar results, each point represents 5% centrality (rightmost: 0-5%; leftmost: 75-80%). The  $p+p$  and Au+Au spectra are taken from [4],  $d$ +Au from [5], Cu+Cu from [6]. HG-PYTHIA simulations modified from [7] are shown as shaded bands. See text for detail.

44 In order to study the dependence of the medium modification of high- $p_T$   
 45 charged hadrons on system size,  $R_{AA}$  for charged hadrons integrated above

46 5.1 GeV/ $c$  is plotted as a function of  $N_{\text{part}}$ . Thanks to the high statistics  
 47 of the Isobar dataset, we perform this analysis in 5%-wide centrality bin.  
 48 Shown in Fig.1,  $R_{AA}$  from Isobar collisions increases gradually from 0-5%  
 49 central to 55-60% peripheral collisions, which aligns with the expectation  
 50 that hard partons experience less quenching as  $N_{\text{part}}$  decreases. When com-  
 51 pared against similar measurements in other collision systems ([4-6]), we  
 52 observe that in this region, similar  $N_{\text{part}}$  leads to similar  $R_{AA}$  regardless of  
 53 the collision system. This corroborates that  $N_{\text{part}}$  is the dominating factor  
 54 in modification of hard partons. The Ru+Ru and Zr+Zr  $R_{AA}$  results are  
 55 consistent with each other within uncertainties.

56 In more peripheral events, one would naively expect smaller quenching  
 57 effects and a larger  $R_{AA}$ . Actually, as cold nuclear matter effects become  
 58 dominant,  $R_{AA}$  in smaller systems (i.e.  $p$ +Pb and  $d$ +Au) has been ob-  
 59 served to be consistent with or even above one at intermediate  $p_T$  [5, 8].  
 60 However, the  $R_{AA}$  values in Isobar collisions with  $N_{\text{part}} < 20$  start to de-  
 61 crease from 60% up to 80% peripheral events, and deviate from previous  
 62 small system measurements. Event selection and geometry biases may con-  
 63 tribute to this deviation, as demonstrated by the HG-PYTHIA [7], which  
 64 shows that the number of hard scatterings per nucleon-nucleon collision is  
 65 smaller in peripheral events, and the effect is significantly stronger when se-  
 66 lecting centrality via experimental observables compared to via the impact  
 67 parameter. This effect is also observed by CMS [9] and ALICE [10]. Here  
 68 we show simulations for the Isobar data using HG-PYTHIA. To maximally  
 69 mimic the experimental condition, we use the number of charged particles  
 70 with  $|\eta| < 0.5$  and  $p_T > 0.2$  GeV/ $c$  as the centrality indicator, calculated  
 71 the invariant yield for charged particles with  $p_T > 5$  GeV/ $c$ , and compared  
 72 to simulated  $p+p$  yield as in real data. The results (shaded bands in Fig. 1)  
 73 qualitatively predict the decrease in  $R_{AA}$  at similar  $N_{\text{part}}$  as that observed  
 74 in data; yet quantitatively it over-predicts the bias. A more accurate pre-  
 75 diction needs more detailed simulation, e.g. inclusion of detector effects, to  
 76 see if quantitative agreements can be reached.

### 77 **3. $p_T$ distribution of identified particles in Isobar collisions**

78 While high- $p_T$  particle yields can indicate hard parton modification in  
 79 the medium, bulk properties of the produced medium, e.g. flow velocity,  
 80 are usually extracted via soft hadron spectra. Because of the well-controlled  
 81 and similar running conditions of the two Isobar species, detector effects and  
 82 systematic uncertainties largely cancel when taking the yield ratios between  
 83 them. Therefore, their raw yield ratio can already provide ample physics  
 84 information.

85 We use the same event sample and centrality selection as in Sec.2, and

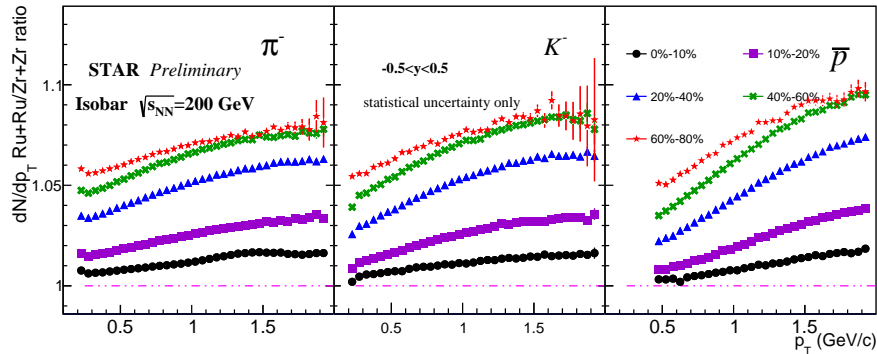


Fig. 2. Mid-rapidity yield ratios of  $\pi^-$ ,  $K^-$  and  $\bar{p}$  between Ru+Ru and Zr+Zr collisions as a function of  $p_T$ , in different centrality classes. Ratios of positive particles show similar trends.

86 follow the particle identification method outlined in Ref. [11] to extract  
 87 identified particle spectra for  $|y| < 0.5$ . As seen in Fig.2, ratios of all species  
 88 show a centrality dependence, with the most central events closest to 1  
 89 and more peripheral events moving up gradually; we also observe the ratio  
 90 increases with  $p_T$ . This is consistent with the Glauber model, which predicts  
 91 larger  $N_{\text{part}}$  and  $N_{\text{coll}}$  ratios between Ru+Ru and Zr+Zr with increasing  
 92 centrality [3]. On the other hand, the Ru+Ru/Zr+Zr ratio of each species  
 93 at a given centrality has subtle differences across  $p_T$ . Namely, the slope for  
 94 protons is larger than that for  $K$  mesons and subsequently  $\pi$  mesons; the  
 95 relationship is similar across centralities. This indicates the trend is driven  
 96 by the difference in the radial flow between Ru+Ru and Zr+Zr collisions.

#### 97 4. Long-range correlations in photonuclear processes

98 A system size scan of QGP signatures would not be considered complete  
 99 without pushing our limits towards smaller systems. In this section,  
 100 we present measurements of long-range correlations in tagged  $\sqrt{s_{\text{NN}}} = 54.4$   
 101 GeV ultra-peripheral Au+Au collisions, in search for signatures of collectiv-  
 102 ity in photonuclear processes. The tagging procedure is applied to select a  
 103  $\gamma$ +Au rich sample, where one nucleus only takes part in the collision by emit-  
 104 ting a virtual photon interacting with the other nucleus, and is achieved by  
 105 taking advantage of the asymmetric nature of the  $\gamma$ +Au processes ([12,13]).

106 In events where the number of tracks detected by the Time Projection  
 107 Chamber (TPC) and matched to the Time of Flight (TOF) detector falls in  
 108 the range of  $1 \leq N_{\text{trk}}^{\text{TOF}} < 8$ , we measure the two-dimensional correlation  
 109 function in relative azimuthal angle  $\Delta\phi$  and relative pseudorapidity  $\Delta\eta$  of

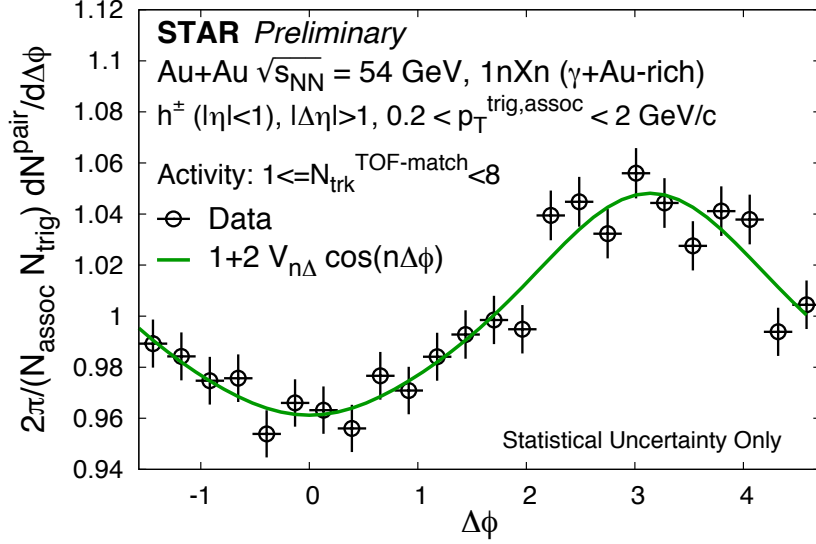


Fig. 3. Long-range azimuthal correlation of charged particles produced in photonuclear processes tagged in 54.4 GeV ultra-peripheral Au+Au collisions.

110 particle pairs. We select TOF-matched tracks as “trigger particles” and  
 111 associate each trigger particle with the remaining tracks with  $|\eta| < 1$  and  
 112  $0.2 < p_T^{\text{trig, assoc}} < 2 \text{ GeV}/c$ . The number of “trigger particles” is denoted as  
 113  $N_{\text{trig}}$ . We obtain the correlation function in  $\Delta\phi$ , integrated over  $|\Delta\eta| > 1$ ,  
 114 and perform a Fourier decomposition as

$$Y(\Delta\phi, |\Delta\eta| > 1) \equiv \frac{2\pi}{N_{\text{trig}} N_{\text{assoc}}} \frac{dN^{\text{pair}}}{d\Delta\phi} = 1 + \sum_n 2V_{n\Delta} \cos(n\Delta\phi), \quad (1)$$

115 where  $V_{n\Delta}$  are the Fourier coefficients,  $n$  is the order of harmonics, and  
 116  $N_{\text{assoc}}$  is the average number of pairs per trigger particle. Figure 3 shows the  
 117 normalized yield  $Y(\Delta\phi)$  and the decomposition. No ridge-like component,  
 118 i.e., a significant  $Y(\Delta\phi)$  enhancement near  $\Delta\phi = 0$  that is considered the  
 119 signature of collectivity, is seen within uncertainties. We aim to extend these  
 120 measurements with high statistics  $\gamma$ +Au-rich event samples using planned  
 121 2023 and 2025 data of Au+Au collisions at  $\sqrt{s_{\text{NN}}} = 200 \text{ GeV}$ , and the  
 122 extended  $\eta$  coverage offered by the STAR forward upgrade [14].

## 123 5. Summary

124 In these proceedings, several studies that improve our understanding  
 125 on the existence and properties of the QGP in different collision systems,

126 and their dependence on initial conditions are presented. We show via the  
 127 Isobar results in combination with other measurements, that inclusive  $R_{AA}$   
 128 of high  $p_T$  hadrons is mostly driven by  $N_{\text{part}}$  regardless of initial geome-  
 129 try. In peripheral events of the Isobar collisions,  $R_{AA}$  is observed to be  
 130 lower than unity, which may be due to event selection and geometry bias  
 131 in the measurement. We also observe that identified particle yield ratios  
 132 between Ru+Ru and Zr+Zr systems show centrality dependence, and the  
 133 slopes of these ratios as a function of  $p_T$  are larger for heavier particles.  
 134 These results demonstrate our sensitivity to the difference between the Iso-  
 135 bar species. We also explore potential collectivity in photonuclear processes  
 136 via tagged ultra-peripheral Au+Au events. No ridge-like structure associ-  
 137 ated with collectivity is found. These studies will help us understand how  
 138 QGP signatures depend on the system size and geometry, and contribute to  
 139 the “system size scan” which will explore the evolution of QGP properties  
 140 with the initial state.

## REFERENCES

- 141 [1] W. Busza, K. Rajagopal, and W. van der Schee, Annual Review of Nuclear  
 142 and Particle Science **68**, 339 (2018).  
 143 [2] STAR, M. M. Aggarwal *et al.*, (2010), 1007.2613.  
 144 [3] STAR, M. S. Abdallah *et al.*, Phys. Rev. C **105**, 014901 (2022).  
 145 [4] STAR, J. Adams *et al.*, Phys. Rev. Lett. **91**, 172302 (2003).  
 146 [5] STAR, J. Adams *et al.*, Phys. Rev. Lett. **91**, 072304 (2003).  
 147 [6] STAR, B. I. Abelev *et al.*, Phys. Rev. C **81**, 054907 (2010).  
 148 [7] C. Loizides and A. Morsch, Physics Letters B **773**, 408 (2017).  
 149 [8] ALICE, B. B. Abelev *et al.*, Eur. Phys. J. C **74**, 3054 (2014), 1405.2737.  
 150 [9] CMS, A. M. Sirunyan *et al.*, Phys. Rev. Lett. **127**, 102002 (2021).  
 151 [10] ALICE, J. Adam *et al.*, Phys. Rev. C **91**, 064905 (2015).  
 152 [11] STAR, L. Adamczyk *et al.*, Phys. Rev. C **88**, 014902 (2013).  
 153 [12] J. D. Brandenburg, N. Lewis, P. Tribedy, and Z. Xu, (2022), 2205.05685.  
 154 [13] STAR collaboration, N. Lewis, These proceedings .  
 155 [14] STAR collaboration, X. Sun, These proceedings .